

# Synthesis and Characterization of NiCo Bimetal Electrocatalyst for Water Splitting

Amarisa Nur Affifah\*, Aulia Rinjani Setiawan, Qori'atun Ni'mah Salsabila

Department of Chemistry, Faculty of Mathematics and Natural Science, Universitas Negeri Jakarta, Jl. Rawamangun Muka, Jakarta 13220, Indonesia

\*Corresponding author: [amarisanur@gmail.com](mailto:amarisanur@gmail.com)

## Received

31 August 2025

## Received in revised form

22 September 2025

## Accepted

04 November 2025

## Published online

29 December 2025

## DOI

<https://doi.org/10.56425/cma.v5i1.119>



© 2025 The author(s). Original content from this work may be used under the terms of the [Creative Commons Attribution 4.0 International License](https://creativecommons.org/licenses/by/4.0/).

## Abstract

This research focuses on developing bimetallic nickel-cobalt (NiCo) electrocatalysts for water-splitting applications via a tailored electrodeposition approach using saccharin as a structure-directing additive. The introduction of saccharin refined the material's crystal size, promoted nickel enrichment in the alloy, and produced a smoother, more porous surface morphology, which collectively enhance the electrochemical active area. The modified catalyst exhibited improved catalytic activity for both hydrogen and oxygen evolution, displaying favorable onset potentials (-0.1593 V for HER and 1.6427 V for OER) and accelerated reaction kinetics, as reflected by Tafel slopes of 134.2 mV/dec and 24.96 mV/dec, respectively. While charge-transfer resistance was not lowered, long-term stability and corrosion resistance were markedly enhanced in the presence of saccharin. These results demonstrate that microstructural engineering through additive-assisted electrodeposition can effectively boost the durability of NiCo electrocatalysts, underscoring the importance of morphology control for sustained performance in energy-conversion systems.

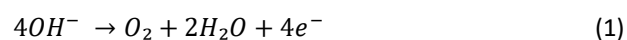
**Keywords:** catalyst, NiCo, additive, saccharin, water splitting

## 1. Introduction

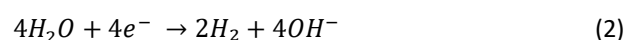
The increasing global demand for energy, coupled with high dependence on CO<sub>2</sub>-emitting fossil fuels, has had a detrimental impact on Earth's natural ecosystems. In response, the global development of renewable energy sources has become crucial, particularly to ensure sustainable progress in developing countries [1]. The continued reliance on conventional fuels raises significant problems related to resource scarcity and the environmental impacts of greenhouse gas emissions, which drive global warming. Therefore, alternative solutions that provide environmentally friendly and sustainable energy sources are urgently needed.

Hydrogen is widely considered an ideal energy carrier due to its high energy density and clean combustion, producing only water (H<sub>2</sub>O) as a byproduct [2]. To overcome the intermittent nature of renewables, hydrogen (H<sub>2</sub>) production via electrocatalytic water

splitting has emerged as a promising and effective solution [3]. Electrochemical water splitting involves two fundamental half-reactions: the oxygen evolution reaction (OER) and the hydrogen evolution reaction (HER) [4]. However, operation in acidic media imposes limitations on electrocatalysts for HER and OER, typically requiring noble metals and metal oxides, which significantly increase the cost of proton exchange membrane (PEM) systems [5]. In contrast, alkaline media allow for a broader selection of electrocatalyst materials and are particularly advantageous for developing OER catalysts [6,7]. In alkaline conditions, OER occurs at the anode:



and HER occurs at the cathode:



Developing efficient electrocatalysts for HER and OER remains a significant challenge, primarily due to their slow reaction kinetics [6]. Pt-based materials are known for

excellent HER performance, while Ru/Ir-based materials excel in OER. Despite their high catalytic activity, the scarcity and high cost of these noble metals hinder their widespread adoption [8]. Therefore, alternative electrocatalysts that are cost-effective, highly active, and scalable are essential. Among various transition metals, iron (Fe), cobalt (Co), nickel (Ni), and molybdenum (Mo) are particularly promising due to their good stability and electrocatalytic activity [9].

Nickel-based materials are widely recognized as effective non-precious electrocatalysts for HER in alkaline media, owing to their favorable activity and low cost. Nickel also exhibits excellent alloying ability with other noble and transition metals in various ratios, enabling the development of bimetallic catalyst systems with enhanced activity and stability compared to pure Ni [10]. To further improve catalytic performance, nickel is often combined with cobalt. Cobalt (Co) has gained considerable attention as a promising non-precious metal due to its well-known catalytic performance in water splitting [11]. Studies have shown that combining different metals can create a synergistic effect, significantly boosting catalytic performance in water splitting systems [12]. Thus, NiCo alloys represent a promising alternative for use as electrocatalysts, as they leverage the complementary properties of nickel and cobalt to achieve higher activity and durability than their single-metal counterparts.

Various synthesis techniques exist, including chemical vapor deposition, hydrothermal synthesis, corrosion methods, and electrodeposition [13]. Among these, electrodeposition offers several key advantages: it enables precise morphological control, is cost-effective and scalable, environmentally benign, and typically yields stable catalysts [14,15]. This method also allows for the adjustment of surface area, electronic properties, and surface reactivity, critical factors influencing catalytic activity. Co and Ni electrodeposition often exhibits co-deposition anomalies, where metal distribution deviates from expected electrochemical behavior [16,17]. Optimizing NiCo electrodeposition therefore relies heavily on the careful adjustment of processing variables, which directly affect composition and material characteristics. Saccharin is widely used as an additive in the electrodeposition of various metals and alloys due to its effectiveness [18,19]. With the molecular formula  $C_7H_5NO_3S$ , saccharin contains sulfur (S), oxygen (O), and carbonyl functional groups, all of which possess lone pairs and  $\pi$  electrons. It has long been employed in nickel plating solutions to refine surface morphology and reduce grain size [20,21]. As such, saccharin has the potential to enhance the efficiency of NiCo electrocatalysts produced via electrodeposition [22].

Based on this background, this study aims to synthesize NiCo material with fine crystallite size and evaluate its effect on electrocatalytic activity. Electrochemical tests were conducted to assess the relationship between crystallite size and charge transfer efficiency, reaction kinetics, and catalyst stability. The addition of saccharin served as a strategy to control crystal growth and achieve a smoother, more uniform morphology.

## 2. Materials and Methods

### 2.1 Synthesis of NiCo thin films

NiCo thin films were synthesized by electrodeposition. An aqueous electrolyte solution was prepared containing 0.08 M nickel(II) sulfate ( $NiSO_4$ ), 0.02 M cobalt(II) sulfate ( $CoSO_4$ ), 0.3 M boric acid ( $H_3BO_3$ ), and 2 g/L saccharin additive. The films were deposited onto a 1 x 2.5 cm copper (Cu) substrate. Electrodeposition was performed at room temperature for 30 minutes at a constant potential of -1.4 V vs. Ag/AgCl, using a Cu working electrode, a Pt wire counter electrode, and an Ag/AgCl reference electrode. A NiCo catalyst was also synthesized without the saccharin additive under identical conditions for comparison.

### 2.2 Characterization

The crystal structure and lattice parameters of the NiCo nanoparticles were analyzed using X-ray diffraction (XRD). The surface morphology of the NiCo films was examined, and the chemical composition was determined by X-ray fluorescence (XRF) spectroscopy.

### 2.3 Linear sweep voltammetry (LSV)

Hydrogen evolution reaction (HER) measurements were performed on the NiCo films in a 0.5 M KOH electrolyte over a potential range of -0.5 V to -1.5 V vs. Ag/AgCl. Oxygen evolution reaction (OER) measurements were conducted in the same electrolyte over a potential range of 0.3 V to 0.8 V vs. Ag/AgCl.

### 2.4 Chronoamperometry (CA)

Chronoamperometry (CA) measurements were carried out on the NiCo films in a 0.5 M KOH electrolyte for 2 hours. Measurements were performed at fixed potentials of 0.8 V and -0.5 V vs. Ag/AgCl, corresponding to the overpotentials for OER and HER, respectively, as determined from the LSV results.

### 2.5 Electrochemical impedance spectroscopy (EIS) and potentiodynamic polarization (PDP)

Electrochemical impedance spectroscopy (EIS) was performed in a 0.5 M KOH electrolyte across a frequency range of 100 kHz to 0.1 Hz. Potentiodynamic polarization (PDP) measurements were conducted in a 3.5 wt% NaCl solution, scanning from -750 mV to 750 mV vs. Ag/AgCl at a rate of 1 mV/s.

### 3. Result and Discussion

The XRD characterization results are shown in Fig 1, which shows five peaks located at  $2\theta$  angles of  $50.7^\circ$ ,  $52^\circ$ ,  $59.2^\circ$ ,  $60.9^\circ$ , and  $89^\circ$ . These correspond to the Miller indices (111), (020), and (022). Based on the graph, the NiCo nanoparticles (NPs) have a cubic crystal structure, where the Ni and Co diffraction peaks overlap at the second position. The characterization results indicate the formation of NiCo NPs, consistent with the NiCo reference [23] and the database pattern listed in Fig 1. The NiCo sample synthesized with the addition of saccharin (red line) displays noticeably sharper and more intense diffraction peaks than the sample without saccharin (black line). This reflects an improvement in crystallinity, suggesting that saccharin promotes a more ordered crystal structure [24].

The addition of saccharin reduced the NiCo crystallite size from 16.6 nm to 15.6 nm, which is essential for expanding the electrochemically active surface area and shortening the transport distance for charge carriers [25,26]. This refinement, coupled with the improved crystallinity and structural ordering induced by saccharin, further enhances the catalyst's porosity and contributes significantly to its overall water-splitting efficiency [27,28]. These beneficial effects arise from the ability of saccharin's functional groups, containing lone pairs and  $\pi$  electrons, to interact with the electrode surface during electrodeposition, resulting in superior film morphology and smoother surfaces [29].

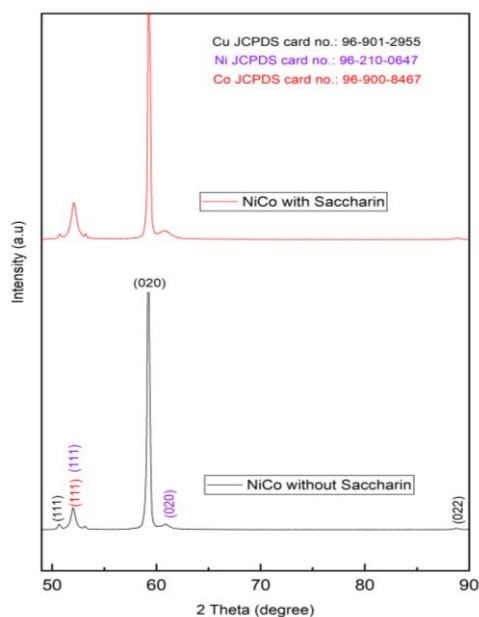
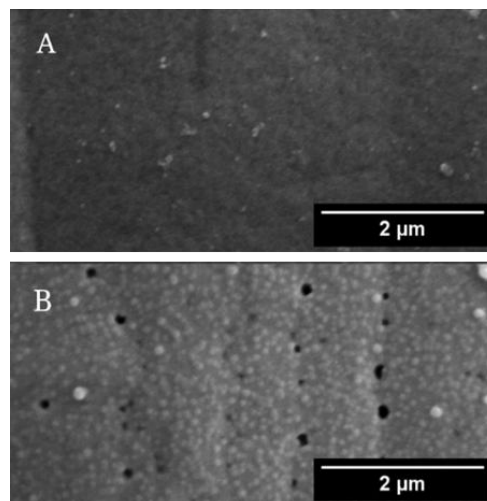


**Figure 1.** XRD patterns of NiCo thin films synthesized with and without saccharin.



SEM analysis was carried out to observe the morphological differences between NiCo samples

**Figure 2.** SEM micrographs of (a) NiCo (b) NiCo with saccharin. prepared with and without saccharin additives. Based on the images, there are significant morphological differences. The morphology of NiCo without saccharin (Fig 2a) has a dense and rough surface, resulting from excessive or uncontrolled synthesis. This can be seen from the darker surface, which indicates a thick NiCo layer. In contrast, the surface morphology of NiCo with saccharin (Fig 2b) shows significant changes, forming more uniform crystals. The brighter surface indicates a thinner and smoother layer with pores that can increase the catalyst's surface area [30]. This positive change is associated with the role of saccharin in encouraging nucleation, thereby controlling crystal formation and producing thinner and more porous grains [31].

**Table 1.** Composition of NiCo thin films synthesized with and without saccharin.

Samples	Composition (%)	
	Co	Ni
NiCo with saccharin	40.911	59.089
NiCo without saccharin	45.177	54.823

XRF testing was performed to determine the elemental composition of the metals in the synthesized material, thus determining the ratio of nickel (Ni) to cobalt (Co) in the NiCo alloy. Based on Table 1, the synthesis of NiCo with the addition of saccharin shows a Ni:Co composition close to a 3:2 ratio. The addition of saccharin resulted in a decrease in the cobalt content in the alloy. This phenomenon is explained by increased adsorption of saccharin on the electrode surface, which can increase cathodic polarization and inhibit the overall metal deposition process [32]. Saccharin has been identified as a crucial additive in

suppressing the anomalous co-deposition behavior characteristic of NiCo systems. Saccharin can modulate the electrodeposition kinetics, thereby promoting Ni incorporation over Co yielding Ni-enriched deposits with enhanced compositional control and improved structural uniformity [33]. Furthermore, other studies have reported that in acetate solutions, saccharin tends to accelerate nickel deposition while simultaneously inhibiting cobalt deposition [34].

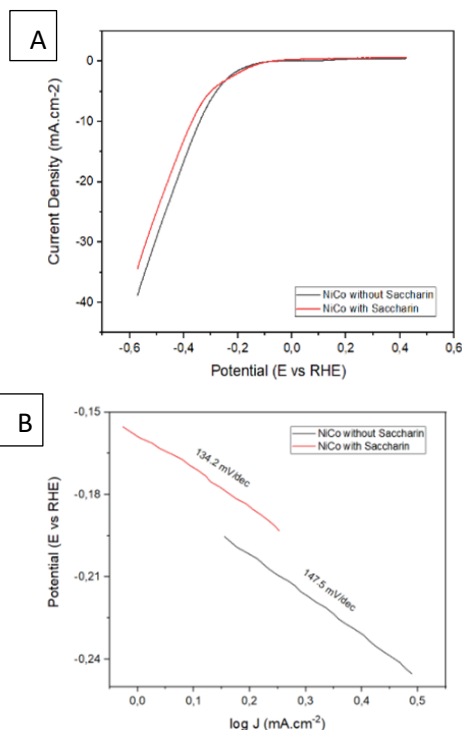


**Figure 3.** (a). LSV curves of HER (b) Tafel plots of HER for NiCo thin films synthesized with and without saccharin in 0.5 M KOH.

HER on the NiCo nanoparticle catalyst with saccharin additive was evaluated under basic conditions in 0.5 M KOH, with a potential range from -1.5 V to -0.5 V. The electrocatalytic activity shows an onset potential of -0.1593 V, as seen in Fig 3, indicating that hydrogen evolution occurs earlier in NiCo NPs with the saccharin additive [35]. The Tafel slope value of 134.2 mV/dec for NiCo NPs with saccharin indicates that the additive effectively increases the catalytic activity. This catalytic activity is also better than that of a previously reported NiCo-LDH catalyst, which had a Tafel slope of 254 mV/dec [36]. However, the overpotential value obtained with saccharin addition was -0.3693 V. NiCo electrodes with finer crystallites showed slightly higher HER overpotential values. This is thought to be related to additive residues from the synthesis process, which can limit ion access to the active electrode surface. Previous research also reported that saccharin can cause an increase in cathodic overpotential because it inhibits the ion reduction process on the electrode surface [37].

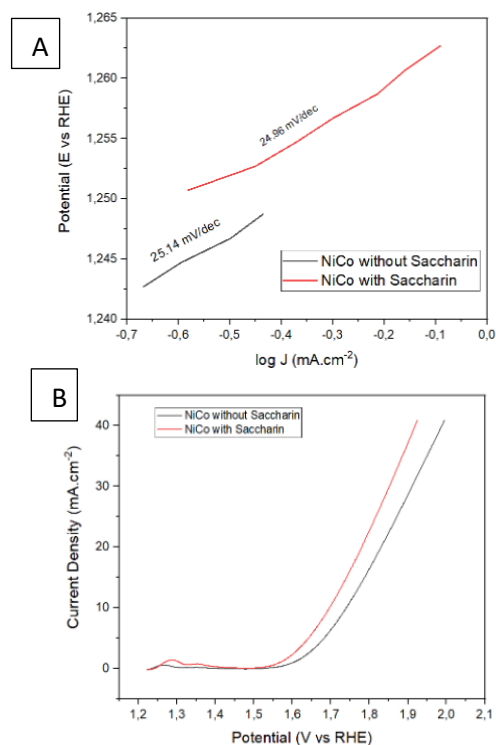


**Figure 4.** (a) LSV curves of OER (b) Tafel plots of OER for NiCo thin films synthesized with and without saccharin in 0.5 M KOH.

OER under the same conditions showed uniform catalyst activity. NiCo NPs with saccharin additives had a Tafel slope value of 24.96 mV/dec, an overpotential at 10 mA·cm<sup>-2</sup> of 0.4627 V, and an onset potential of 1.6427 V. This indicates good reaction kinetics, as seen from the NiCo catalyst under conditions without saccharin additives in Fig 4, when used as a bifunctional electrode for water splitting [38]. These test results explain that catalytic activity can be controlled by size, shape, composition, and interface and surface engineering.

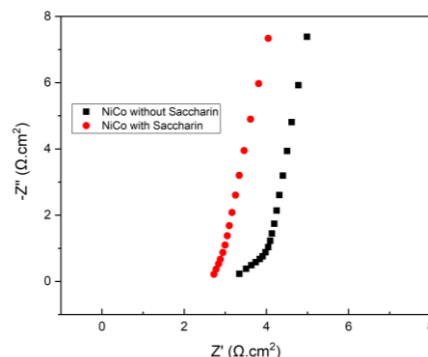


**Figure 5.** Nyquist plot of NiCo thin films synthesized with and without saccharin in 0.5 M KOH.

In Fig 5, the Nyquist plot obtained from EIS measurements shows a low charge transfer resistance ( $R_{ct}$ ), indicating efficient electron transfer and improved electrochemical kinetics. The NiCo catalyst with saccharin shows a lower charge transfer resistance (1.40  $\Omega$ )

compared to the catalyst prepared without saccharin (2.85  $\Omega$ ). The smaller semicircle size reflects better charge transfer, allowing electrons to move more efficiently between the electrode surface and electrolyte species, thus improving overall catalytic performance [23]. Although crystallite size fineness can affect morphology, it does not always directly correlate with faster kinetics. Therefore, other factors are suspected to influence reaction kinetics, such as the balance between crystallite size and electronic conductivity, which is crucial for optimizing catalytic performance.

Chronoamperometry stability tests were conducted at fixed HER (-0.56 V) and OER (0.8 V) potentials for 2 hours. The saccharin-modified NiCo catalyst retained 80.6% of its initial OER current and 45.76% of its HER current (Fig 6b), demonstrating superior long-term stability compared to the additive-free sample. These results indicate that the NiCo catalyst with saccharin additive has better stability compared to NiCo without additives. The improved stability can be ascribed to the role of saccharin in reducing residual stress and improving film quality, resulting in a more homogeneous and compact layer that is resistant to degradation under long-term electrochemical operation [19]. Similar observations have been reported in previous studies, where the addition of saccharin during electrodeposition resulted in smaller crystallite sizes and increased structural stability of metal alloy catalysts [39].

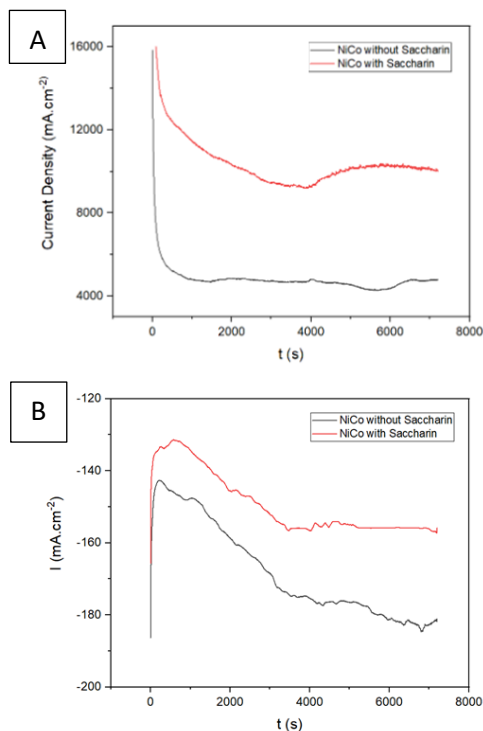


**Figure 6.** Chronoamperometric test of (a) OER (b) HER for NiCo thin films synthesized with and without saccharin in 0.5 M KOH.

In the PDP test, the corrosion potential ( $E_{corr}$ ) and corrosion current density ( $i_{corr}$ ) values were obtained from polarization measurements [40]. The corrosion potential  $E_{corr}$  indicates the thermodynamic tendency of a metal to corrode under certain environmental conditions. A more positive  $E_{corr}$  value indicates a lower tendency for corrosion, while a more negative  $E_{corr}$  value indicates a greater thermodynamic driving force for corrosion [41].

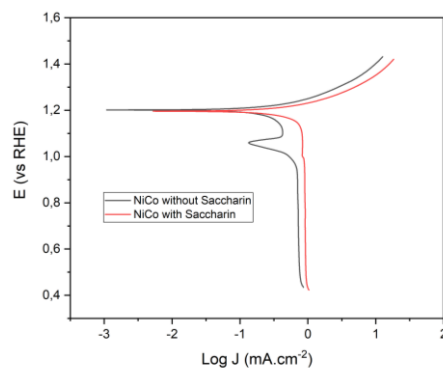


**Figure 7.** Potentiodynamic polarization curve of NiCo thin films synthesized with and without saccharin in 3.5 wt% NaCl.

**Table 3.**  $i_{corr}$  and  $E_{corr}$  potentiodynamic polarization for NiCo thin films synthesized with and without saccharin.

Sample	$i_{corr}$ (mA.cm <sup>-2</sup> )	$E_{corr}$ (V)
NiCo with saccharin	1.2	-2.97
NiCo without saccharin	1.19	-2.28

Additionally, the corrosion current density  $i_{corr}$  represents the corrosion rate from a kinetic perspective. A lower  $i_{corr}$  value indicates a slower metal dissolution rate, reflecting better corrosion resistance [42]. The  $E_{corr}$  and  $i_{corr}$  values were better for NiCo with the addition of saccharin, as shown in Table 3. These results indicate that the NiCo catalyst with saccharin additives has better corrosion resistance because the morphological changes on the NiCo surface become smoother, as shown in Fig 7. These findings align with previous studies explaining that smaller nanoparticle sizes influence corrosion resistance [43]. The measured values of corrosion potential and corrosion current density help to understand how the material behaves when exposed to a corrosive environment [44].

#### 4. Conclusion

The addition of saccharin additives in the synthesis of NiCo successfully produced higher crystallinity with a crystallite size of 15.6 nm, smaller than NiCo without saccharin (16.6 nm), and an increase in nickel content in the alloy. The increase in surface area is also supported by surface morphology results that the addition of saccharin additives significantly smoothens the surface, resulting in

uniform crystal size and pore formation compared to NiCo without saccharin. This is because saccharin additives control the growth of NiCo crystals, thereby increasing electrochemical stability and corrosion resistance, as indicated by chronoamperometry and potentiodynamic polarization tests. However, the higher HER overpotential values and charge transfer resistance in samples with saccharin indicate that a finer crystallite structure does not necessarily improve the kinetic efficiency of electrochemical reactions. Morphology engineering through crystallite size control can be an effective strategy to improve the durability and stability of electrocatalysts in water-splitting applications.

### Author contributions

**Amarisa Nur Affifah:** investigation, formal analysis, writing-original draft. **Aulia Rinjani Setiawan:** investigation, formal Analysis, writing-original draft. **Qori'atun Ni'mah Salsabila:** formal analysis, supervision.

### Conflicts of interest

There are no conflicts to declare.

### Acknowledgements

The authors would like to thank the DRTPM Kemendikbudristek for supporting this research under the National Competitive Applied Research scheme.

### References

- [1] Nejat, P., Jomehzadeh, F., Taheri, M. M., Gohari, M., & Majid, M. Z. A. (2015). A global review of energy consumption, CO<sub>2</sub> emissions and policy in the residential sector (with an overview of the top ten CO<sub>2</sub> emitting countries). *Renewable and sustainable energy reviews*, 43.
- [2] Wang, P., Jia, T., & Wang, B. (2020). A critical review: 1D/2D nanostructured self-supported electrodes for electrochemical water splitting. *Journal of Power Sources*, 474, 228621.
- [3] You, B., & Sun, Y. (2018). Innovative strategies for electrocatalytic water splitting. *Accounts of chemical research*, 51(7), 1571-1580. 62.
- [4] Seh, Z. W., Kibsgaard, J., Dickens, C. F., Chorkendorff, I. B., Nørskov, J. K., & Jaramillo, T. F. (2017). Combining theory and experiment in electrocatalysis: Insights into materials design. *Science*, 355, 1-12.
- [5] Hu, C., Zhang, L., & Gong, J. (2019). Recent progress made in the mechanism comprehension and design of electrocatalysts for alkaline water splitting. *Energy & Environmental Science*, 12(9), 2620-2645.
- [6] Chen, Z., Duan, X., Wei, W., Wang, S., & Ni, B. J. (2019). Recent advances in transition metal-based electrocatalysts for alkaline hydrogen evolution. *Journal of Materials Chemistry A*, 7(25), 14971-15005.
- [7] Zhang, L., Xiao, J., Wang, H., & Shao, M. (2017). Carbon-based electrocatalysts for hydrogen and oxygen evolution reactions. *Acs Catalysis*, 7(11), 7855-7865.
- [8] Kuang, P., & Yu, J. (2022). Graphene oxide-based materials in electrocatalysis. In *Graphene Oxide-Metal Oxide and other Graphene Oxide-Based Composites in Photocatalysis and Electrocatalysis. Elsevier*. 189-238.
- [9] Batool, M., Hameed, A., & Nadeem, M. A. (2023). Recent developments on iron and nickel-based transition metal nitrides for overall water splitting: A critical review. *Coordination Chemistry Reviews*, 480, 215029.
- [10] Miao, Z., Xu, C., Zhan, J., & Xu, Z. (2021). Morphology-control and template-free fabrication of bimetallic Cu-Ni alloy rods for ethanol electro-oxidation in alkaline media. *Journal of Alloys and Compounds*, 855, 157438.
- [11] Wang, J., Cui, W., Liu, Q., Xing, Z., Asiri, A. M., & Sun, X. (2016). Recent progress in cobalt-based heterogeneous catalysts for electrochemical water splitting. *Advanced materials*, 28(2), 215-230.
- [12] Yanli, G., Yun, Z., Xiaolong, S., & Bo, L. (2021). The synergistic effect of NiCo nanoparticles and metal organic framework: Enhancing the oxygen evolution reaction of carbon nanohorn-based catalysts. *Journal of Alloys and Compounds*, 885, 160889.
- [13] Liu, J., Zhu, D., Zheng, Y., Vasileff, A., & Qiao, S. Z. (2018). Self-supported earth-abundant nanoarrays as efficient and robust electrocatalysts for energy-related reactions. *Acs Catalysis*, 8(7), 6707-6732.
- [14] Kim, J., Kim, H., Han, G. H., Hong, S., Park, J., Bang, J. & Ahn, S. H. (2022). Electrodeposition: An efficient method to fabricate self-supported electrodes for electrochemical energy conversion systems. In *Exploration* 2(3). 20210077).
- [15] Pi, Y., Shao, Q., Wang, P., Lv, F., Guo, S., Guo, J., & Huang, X. (2017). Trimetallic oxyhydroxide coraloids for efficient oxygen evolution electrocatalysis. *Angewandte Chemie*, 129(16), 4573-4577.
- [16] Liu, J., Zhu, D., Zheng, Y., Vasileff, A., & Qiao, S. Z. (2018). Self-supported earth-abundant nanoarrays as efficient and robust electrocatalysts for energy-related reactions. *Acs Catalysis*, 8(7), 6707-6732
- [17] Bai, A., Hu, C. C., & Wen, T. C. (2003). Composition control of ternary FeCoNi deposits using cyclic voltammetry. *Electrochimica acta*, 48(17), 2425-2434.
- [18] Pellicer, E., Varea, A., Pané, S., Sivaraman, K. M., Nelson, B. J., Suriñach, S., & Sort, J. (2011). A comparison between fine-grained and nanocrystalline electrodeposited Cu-Ni films.

- Insights on mechanical and corrosion performance. *Surface and Coatings Technology*, 205(23-24), 5285-5293.
- [19] Hassani, S., Raeissi, K., & Golozar, M. A. (2008). Effects of saccharin on the electrodeposition of Ni-Co nanocrystalline coatings. *Journal of Applied Electrochemistry*, 38, 689-694.
- [20] Fix, G. L., & Pollack, J. D. (1980). Determination of saccharin in watts nickel plating solutions by first derivative ultraviolet spectrometry. *Analytical Chemistry*, 52(11), 1589-1592.
- [21] Mosavat, S. H., Bahrololoom, M. E., & Shariat, M. H. (2011). Electrodeposition of nanocrystalline Zn-Ni alloy from alkaline glycinate bath containing saccharin as additive. *Applied Surface Science*, 257(20), 8311-8316.
- [22] Kim, Y., Jun, S. E., Lee, G., Nam, S., Jang, H. W., Park, S. H., & Kwon, K. C. (2023). Recent Advances in Water-Splitting Electrocatalysts Based on Electrodeposition. *Materials*, 16(8), 3044.
- [23] Raveendran, M. N., & Hegde, A. C. (2022). Anomalous codeposition of NiCo alloy coatings and their corrosion behaviour. *Materials Today: Proceedings*, 62, 5047-5052.
- [24] Z.Q. Li, C.J. Lu, Z.P. Xia, Y. Zhou, Z. Luo. (2007). X-ray diffraction patterns of graphite and turbostratic carbon. *Carbon*, 1686-1695.
- [25] C. Burda, X.B. Chen, R. Narayanan, M.A. El-Sayed, Chemistry and properties of nanocrystals of different shapes. *Chemical Reviews*, 105 (2005) 1025-1102.
- [26] T.W. Kim, K.-S. Choi, Nanoporous BiVO<sub>4</sub> Photoanodes with Dual-Layer Oxygen Evolution Catalysts for Solar Water Splitting. *Science*, 343 (2014) 990-994.
- [27] Lukic, S., Menze, J., Weide, P., Busser, G. W., Winterer, M., & Muhler, M. (2017). Decoupling the Effects of High Crystallinity and Surface Area on the Photocatalytic Overall Water Splitting over  $\beta$ -Ga<sub>2</sub>O<sub>3</sub> Nanoparticles by Chemical Vapor Synthesis. *ChemSusChem*, 10(21), 4190-4197.
- [28] Loto, R. T., & Babalola, P. (2018). Effect of alumina nano-particle size and weight content on the corrosion resistance of AA1070 aluminum in chloride/sulphate solution. *Results in Physics*, 10, 731-737.
- [29] Choi, J. I., Park, I., Park, S., Yi, M. J., Jang, W., & Seo, J. H. (2025). Kinetic analysis of Nico electrodeposition with saccharin using electrochemical impedance spectroscopy. *Electrochemistry Communications*, 175, 107912.
- [30] Ignatova, Katya & Marcheva, Yordanka. (2016). Effect of saccharine on the properties of Ni-Co alloy coatings deposited in citrate electrolytes. 1-4. 10.1109/ET.2016.7753486.
- [31] Jae-Ik Choi, Inyeol Park, Suyeon Park, Min Jun Yi, Wonbong Jang, Jong Hyun Seo. 2025. Kinetic analysis of Nico electrodeposition with saccharin using electrochemical impedance spectroscopy. *Electrochemistry Communications*. 175.
- [32] Y.F. Yang, B. Deng, Z.H. Wen. (2011). Preparation of Ni-Co alloy foils by electrodeposition. *Advances in Chemical engineering and science*, Vol. 1, pp. 27-32.
- [33] Budi, S., & Manaf, A. (2021). The effects of saccharin on the electrodeposition of NiCoFe films on a flexible substrate. *Materials Research Express*, 8(8), 086513.
- [34] K. R. Marikkannu, G. Paruthimal Kalaigan, T. Vasudevan (2007). The role of additives in the electrodeposition on nickel-cobalt alloy from acetate electrolyte, *J. Alloy and Compounds*, Vol. 438, pp. 332-336
- [35] Liu, X., & Zangari, G. (2001). High moment FeCoNi alloy thin films fabricated by pulsed-current electrodeposition. *IEEE transactions on magnetics*, 37(4), 1764-1766.
- [36] Magar, H. S., Hassan, R. Y. A., & Mulchandani, A. (2021). Electrochemical Impedance Spectroscopy (EIS): Principles, Construction, and Biosensing Applications. *Sensors*, 21(19), 6578.
- [37] Li, Y., Yao, J., & Huang, X. (2016). Effect of Saccharin on the process and properties of nickel electrodeposition from sulfate electrolyte. *Int. J. Metall. Mater. Eng*, 2(123), 2455-2372.
- [38] Kazempour, A., Moradi-Alavian, S., Ashassi-Sorkhabi, H., & Asghari, E. (2025). Synergistic Fe-Mn-Cu ternary alloys enhance bifunctional activity and stability for alkaline water splitting. *Scientific Reports*, 15(1), 1-16.
- [39] Mulmeyda, R., Sidik, A. G., Maura, C. S., & Fazri, A. A. (2024). The Effect of Saccharin on SnNi Alloy: the Electrodeposition and its Electrocatalytic Activity in Ethanol Oxidation Reaction. *Chemistry and Materials*, 3(3), 107-115.
- [40] Wu, Y., Wu, H., Wu, L., Xie, Z. H., Liu, L., Dai, X., ... & Pan, F. (2020). Influence of electrolyte temperature on morphology and properties of composite anodic film on titanium alloy Ti-10V-2Fe-3Al. *Coatings*, 10(11), 1109.
- [41] Jegdić, B., Radojković, B., Bobić, B., Krmar, M., & Ristić, S. S. (2018). Corrosion resistance of metalized layers on steel parts in ventilation mill. *Metallurgical and Materials Engineering*, 24(2), 123-132.
- [42] Yuan, J., Wang, Y., Xing, Z., Zhao, G., Hou, X., Zhong, J., & Tan, D. (2024). Correlation between grain orientation and corrosion performance of different tantalum crystal facets in 3.5 wt% NaCl aqueous solution. *International Journal of Electrochemical Science*, 19(10), 100777.
- [43] Aslam, R. (2023). Potentiodynamic polarization methods for corrosion measurement. In *Electrochemical and Analytical Techniques for Sustainable Corrosion Monitoring* (pp. 25-37). Elsevier.

- [44] Uli, R., Saputera, W. H., Sasongko, D., & Devianto, H. (2025). Development of Tungsten Oxide (WO<sub>3</sub>) Based Catalyst for Degradation of Palm Oil Mill Effluent (POME) with Photocatalytic Technology. *Jurnal Teknik: Media Pengembangan Ilmu dan Aplikasi Teknik*, 24(1), 34-42.